Washington University in St. LLouis

The following report from Washiaington University for the period contains these brief chapters:

Objectives for the Third Budget YYear
Outline of Accomplishments

1. Turbulence Parameters in n 18-in. Diameter Columns with and
    without Internals
2. Establishment of the Relatationship between the Axial Dispersion
    Coefficient and Parameterers of the Phenomenological Recycle
    with Cross Flow and Eddyly Diffusion Model
3. Progress in Evaluation of f the Momentum Balance Equation
    for Bubble Column Usingg CARPT and CT Measurements

ENGINEERING DEVELOPMENT OF
SLURRY BUBBLE (COLUMN REACTOR (SBCR) TECHNOLOGY

Eleventh Quarterly Report

Budgetet Year 3: October 1 - December 31, 1997

Submitted to

ı Air Products and Chemicals, Inc.

Ccontract No.: DE-FC 22 95 PC 95051

Chemmical Reaction Engineering Laboratory
CChemical Engineering Department
VWashington University in St. Louis

Objectives for the Third Budget Year

The main goal of this subcontract from the Department of Energy via Air Products to the Chemical Reaction Engineering L Laboratory (CREL) at Washington University is to study the fluid dynamics of slurry bubble ccolumns and address issues related to scaleup and design. The objectives for the third budget yeaar (October 1, 1997 – September 30, 1998) were set as follows:

- Further development of phenaomenological models for liquid and gas.

- Testing of the models against it available data from the LaPorte AFDU.

- Evaluation of turbulent paranmeters in 18-in.-diameter columns with and without internals using collected CARPT data i. in these columns.

- Development of relationships is between fundamental and simpler practical models for industrial use.

- Further improvement in fundalamental computational fluid dynamics models and testing of the models against the CARPT/CCT data.

- Preliminary assessment of diffferences in gas-liquid and gas-liquid-solid systems.

- Testing of the effect of the disistributor on flow patterns.

In this report, the research progreess and achievements accomplished in the eleventh quarter (October 1 - December 31, 1997)') are discussed.

Outline of Accomplishments

- **Turbulence Parameters in 118-in. Diameter Columns with and without Internals**

The turbulence parameters (normaal and shear stresses and kinetic energy) were evaluated from Computer Automated Radioactivwe Particle Tracking (CARPT) experiments performed at 2, 5 and 10 cm/s superficial gas velocities.s. These experiments were conducted with the air-drakeoil system in a 44.0-cm (18-in.) diammeter column with and without internals. The internals consisted of 16 tubes of 1-in. diameter, whiaich simulate the heat exchanger in the 18-in. diameter column used in the AFDU at LaPorte, Texxas. A perforated plate distributor with hole diameter equal to 0.77 mm and an open area equal t to 0.076% was used.

The results and comparison betweeen the parameters obtained are reported and discussed.

- **Establishment of the Relaationship between the Axial Dispersion Coefficient and Parameters of the Phenonmenological Recycle with Cross Flow and Eddy Diffusion Model**

A Taylor-type analysis of the tvtwo-dimensional convection-diffusion model for liquid mixing in a bubble column (which was devveloped and reported in the seventh and eighth quarterly reports) was performed to establish a reielationship between the axial dispersion coefficient and the parameters of this new phenommenologically based model. While the recycle with the cross-flow model describes the phenomenaa that contribute to liquid mixing in a bubble column more reasonably than the axial dispeiersion model (ADM), the existence of only one parameter (the axial dispersion coefficient) renders t the ADM still attractive to many. Therefore, we have developed a procedure to estimate the axial dispersion coefficient from the parameters of the phenomenologically more correrect model.

- **Progress in Evaluation of f the Momentum Balance Equation for Bubble Columns Using CARPT and CT Measureiements**

It was reported in the 10th quartrterly report that the addition of the turbulent drag force to the radial momentum balance imprroved the agreement between the R.H.S. and L.H.S. of the balance for the case of high superficial j gas velocity (12 cm/s in 14-cm diameter column). However, for the cases of low superficial gasis velocity (4.8 cm/s) in the 14- and 19-cm diameter columns, the agreement between the R.H.S a and L.H.S. of the radial momentum balance deteriorated with the addition of the turbulent drag fcforce.

In this work, possible sources oof the observed discrepancies are evaluated and discussed. Additional investigations were e also conducted to detect the possible sources of error related to the assumption of fully developped flow and variability in determination of the Reynolds stress and gas holdup profiles, as welltll as the uncertainty in estimation of the gas velocity profile.

TABLE OF CONTENTS

1. Turbulence Parameters in 18-in. Diameter Columns with and without Internals

In the 10th quarterly report, we didiscussed the liquid recirculation velocities obtained by Computer Automated Radioactive Particle TTracking (CARPT) experiments and the cross-sectional gas holdup distribution obtained by CComputer Tomography (CT) for the air-drakeoil system in 18-in. diameter columns with and withoiout internals. Similarities and differences between liquid velocities in the two columns werere discussed. In summary, the time averaged axial liquid velocity profiles in the column wivith internals exhibit trends similar to those obtained in the column without internals. Howevver, as the superficial gas velocity increases, the velocity inversion point seems to move raadially away from the wall in the column with internals, whereas in the column without internals ththe velocity inversion point occurs almost at the same radial position at all gas velocities. In tfthe center of the column, the time-averaged axial velocity in the column with internals is somewhaat larger than that obtained in the same column without internals. This difference could bbe caused by the poor statistics in the center of the column, which at that location is based onn the smallest compartment for counting of the CARPT particle visits and causes increased and ernror in the estimated velocity. Therefore, in the first approximation (in the range of thdie gas superficial velocities studied, 2 to 10 cm/s), the internals do not seem to notably affect liquuid recirculation. However, in the column with internals, the flow becomes developed at a relatatively longer distance from the distributor compared to that in the column without internals.

In this section, the turbulence pararameters (normal and shear stresses and kinetic energy) are evaluated in the same column opoerated with and without internals. The comparison between the obtained parameters is discussed.l.

1.1 Outline of the Experimentss
The experimental setup and condiditions were similar to those reported in the last quarterly report (see Figure 1.1). The column wasas made of Plexiglas with a diameter of 18 inches and a height of 8 feet (L/D=5.3). The distributorr used was a perforated plate with holes 0.77 mm in diameter and an open area of 0.076%. Theie internals were composed of two bundles of 1-in. aluminum tubes. Each bundle had eight equiually distributed tubes. The configuration of the internals simulated the heat exchanger tuboes in the 18-in. diameter slurry bubble column reactor used in LaPorte, Texas. The radioactive p particle used as tracer was Sc 46, with activity of about 350 μCi. Thirty NaI scintillation deteectors were employed in CARPT experiments. Data collection, at each gas superficial velocity, lalasted about 40 hours in order to obtain good statistical results. The experiments were conducted 1 at the gas superficial velocities of 2, 5 and 10 cm/s for the same column with and without internalsls. The system used was air-drakeoil (Drakeol[®] 10, Van Waters & Rogers Inc.).

1.2 Experimental Results and I Discussion

1.2.1 Turbulent Parameters in 1 the Column without Internals
Figures 1.2(a), (b) and (c) show ththe time-averaged shear stress and radial and axial normal stresses in the column without intnternals. It should be noted that the plots were obtained by averaging values over the developped flow region, which occupied the column between the

heights of 30 and 180 cm from n the distributor. The stresses increased with superficial gas velocity, as expected. The trennds were similar to those obtained in the air-water system and in the smaller diameter columns. ' The magnitude of the radial normal stress was about half of that of the axial normal stress, whilele the magnitude of the shear stress was much smaller than that of normal stresses. The figures alslso show that at low superficial gas velocities (2 and 5 cm/s), the axial normal stress was slightlyy larger near the center and near the wall, while at high gas velocity (10 cm/s), the axial normal streress decreased with decreasing distance to the wall, except at the closest point to the wall. This u uncertainty is caused by lack of data near the wall. The magnitude of the radial normal stress at allll three gas velocities slightly increased from the center to the wall. On the other hand, the shear strtresses showed a maximum value near the dimensionless radius (r/R) of 0.5 - 0.6 and almost zerzro near the center and near the wall of the column. All of these observations are similar to thosese obtained in the same size column for the air-water system.

Figure 1.3 shows the turbulent l kinetic energy in the 18-in. diameter column for air-water and air-drakeoil systems and in the 6-inin. diameter column for the air-water system. It is obvious that the turbulent kinetic energy was abbout the same for air-water and air-drakeoil systems, except in the region near the wall, which couiuld also be due to inadequate statistics, causing the error in time averaging. Turbulent kinetic emnergy was higher in the 18-in. column compared to that obtained in the 6-in. diameter column (ththe distributor used in the 6-in. column consisted of a hole size = 0.04 cm and an open area = 0.005%).

1.2.2 Turbulent Parameters s in the Column with Internals
Figures 1.4(a), (b) and (c) illuststrate the time-averaged shear stress and radial and axial normal stresses. As mentioned in the l 10th quarterly report, since a larger distance was needed to develop the flow in the column with inteternals, only the top half of the column was considered to be the developed region, and averaginng was performed only in this part of the column. The trends of axial and radial normal stressess were quite similar to those obtained in the column without internals. The stresses increaseed with gas superficial velocities. However, at 2 cm/s gas superficial velocity, the axial naormal stress increased significantly near the wall, and was even higher than the axial normal strcress at 5 cm/s gas superficial velocity. The reason for this is not clear. For the shear stress, negagative values were observed at gas superficial gas velocities of 2 and 5 cm/s near the wall, even i in the time-averaged sense.

1.2.3 Comparison of Turbuleent Stresses in the Columns with and without Internals
Figures 1.5, 1.6, and 1.7 compaoare the stresses in the columns with and without internals at superficial gas velocities of 2, 5 5 and 10 cm/s, respectively. Figure 1.8 compares turbulent kinetic energy at 10 cm/s gas superficieial velocity, with and without internals. The magnitudes and the trends of the radial profiles of tl the turbulent stresses in the column with internals were quite similar to those obtained in the e column without internals, except near the wall of the column. These differences in the region n near the wall were likely caused by the error associated with the reconstruction of the instantaneieous particle positions and by lack of data. The magnitude of the radial normal stress in the colurmn without internals was slightly higher than that in the column with internals in the region betvtween the column center and the wall, while a reverse trend was observed near the wall of the ccolumn. However, the shear stress in the column with internals was lower than that in the colurmn without internals, indicating that the presence of the internals

indeed reduces the radial length s scales of turbulence. This qualitatively verifies Degalessan's assumption for the LaPorte Altermative Fuels Development Unit reactor (Degalessan, 1997). Of course, comparison of eddy diffuusivities in the columns with and without internals is needed. Since, evaluation of eddy diffusivivities for CARPT data is a very lengthy and time-consuming process, it will be accomplished d during the next phase of the work and cannot be reported here.

In summary, the presence of interernals does not notably change the gross time-averaged flow pattern or turbulent stresses in theie fully developed region of the column, especially at high superficial gas velocity, when theie column is in the churn turbulent regime. Slightly larger differences are observed at the ce:enter and near the wall of the column in some cases, which might result from the poor statistics of p particle occurrence in these regions.

1.3 References

1. Degaleesan, S., "Fluid Dynammic Measurements and Modeling of Liquid Mixing in Bubble Columns," D. Sc. Thesis, Wa:ashington University in St. Louis, 1997.

Detectors

Distributor
(Perforated Plate
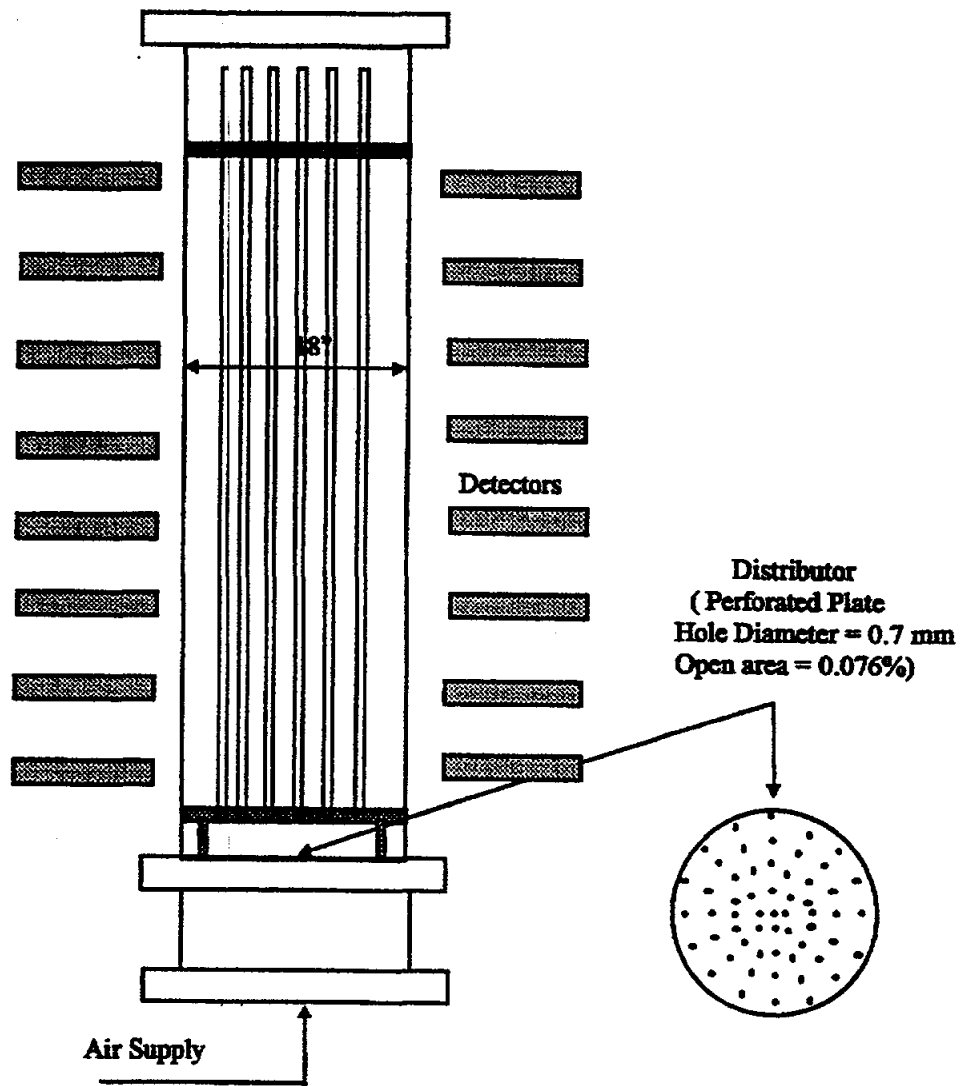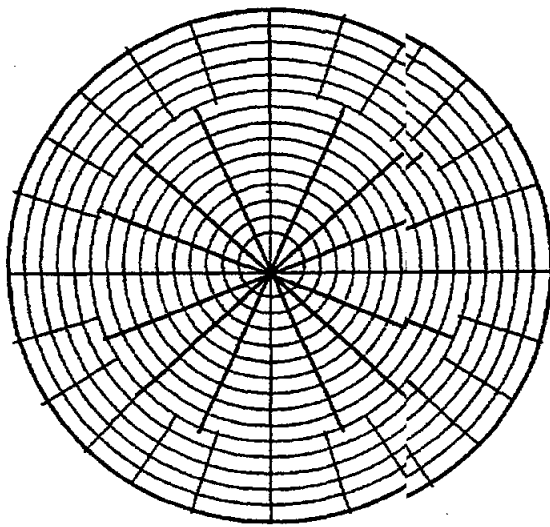Hole Diameter = 0.7 mm
Open area = 0.076%)

Air Supply

Figure 1.1(a). Experirimental set-up for the 18" column CARPT runs

Open area = 0.076%

301 holes of 0.7 mm in diameter on 14 concentric circular rings at 1.5 cm apart.

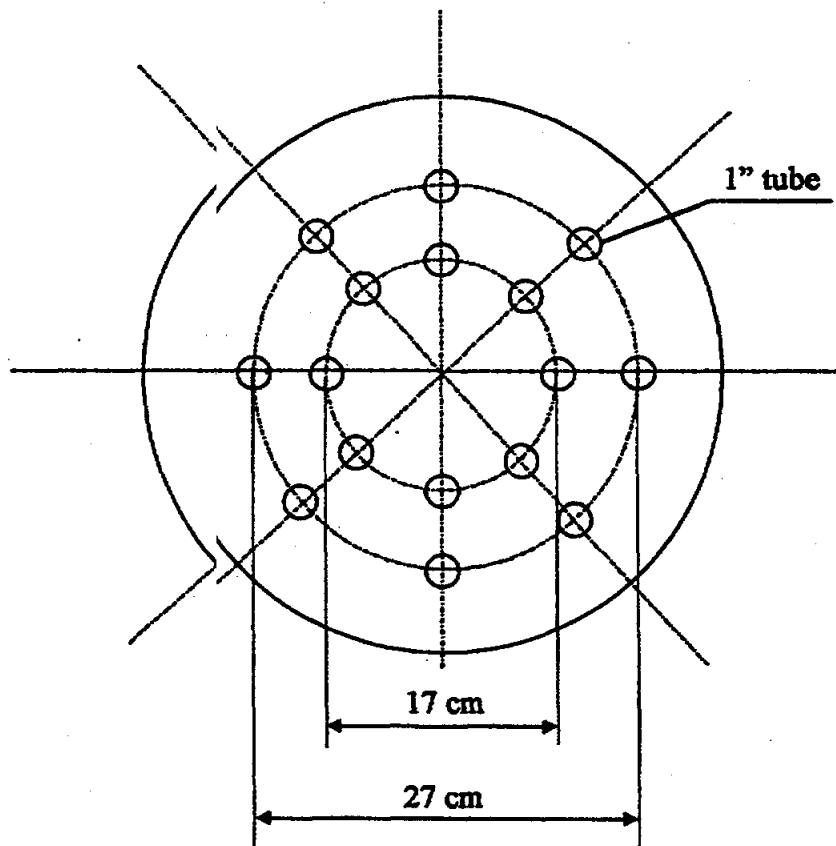Figure 1.1(b). Perforsrated plate distributors used in the experiments

1" tube

17 cm

27 cm

Figure·e 1.1(c). Configuration of the internals
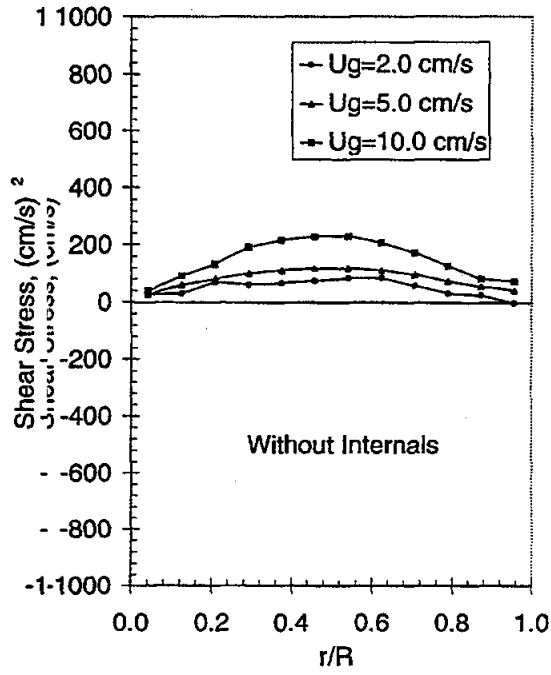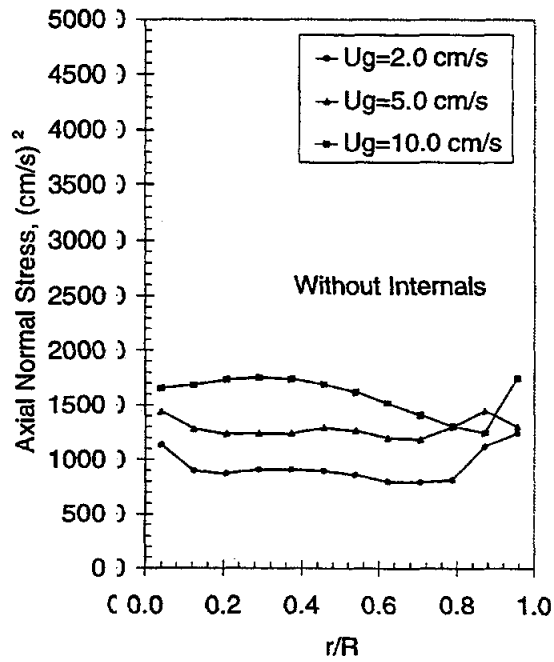
(a)   (b)

(c)

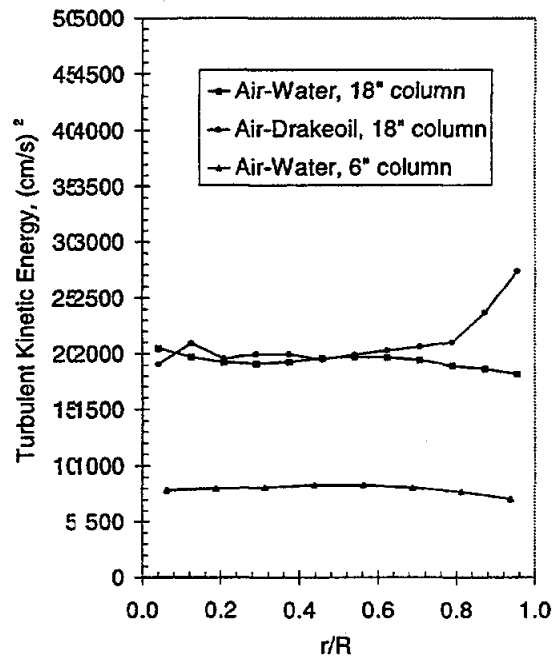**Figure 1.2 Turbulent Parameters in the 18-in. Column without Internals
Using the Air-Drakeoil System**

Figure 1.3 Turbulent Kinetic Energy in 18-in. and 6-in. Diameter Columns (The distributors are: 6-in. c diameter column: hole size = 0.04 cm, open area = 0.05%; 18in. diameter coblumn: hole size = 0.077 cm, open area = 0.076%)
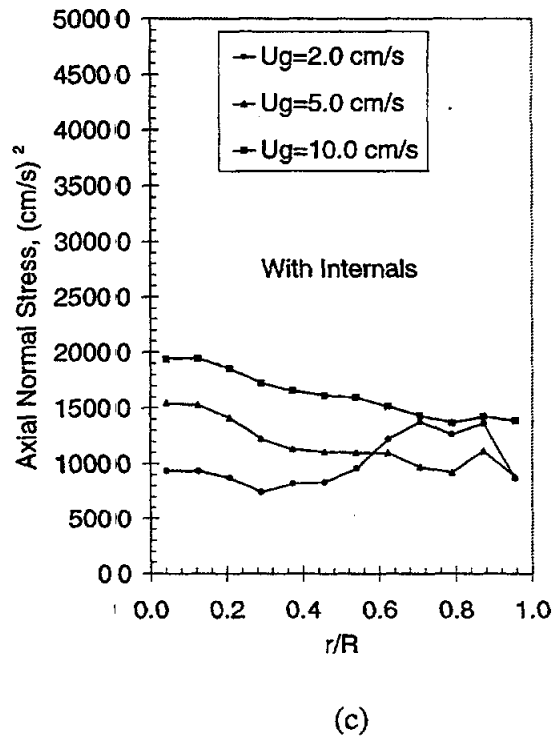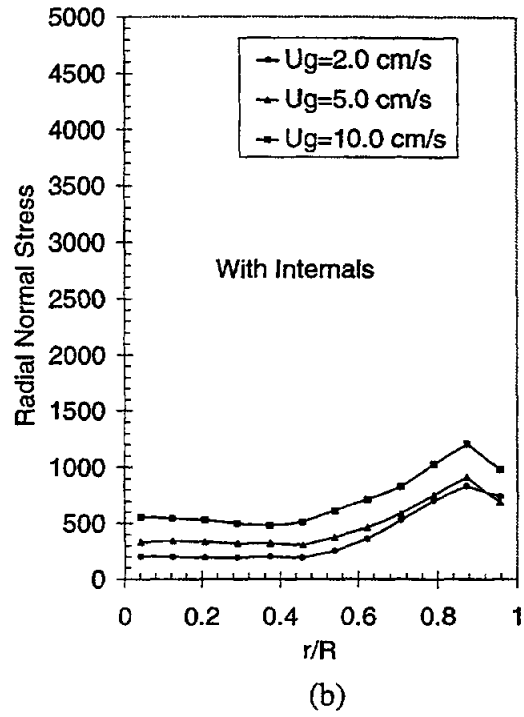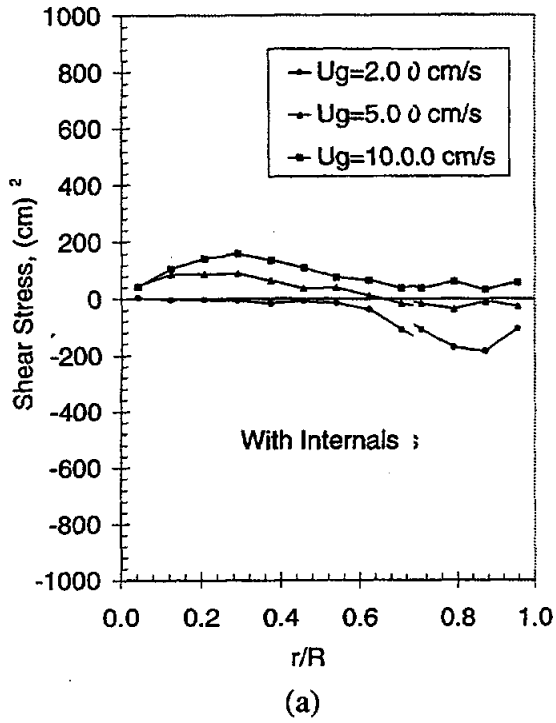
(a)

(b)

(c)

**Figure 1.4 Turbulslent Parameters in the 18-in. Column with Internals
Using the Air-Drakeoil System**

24
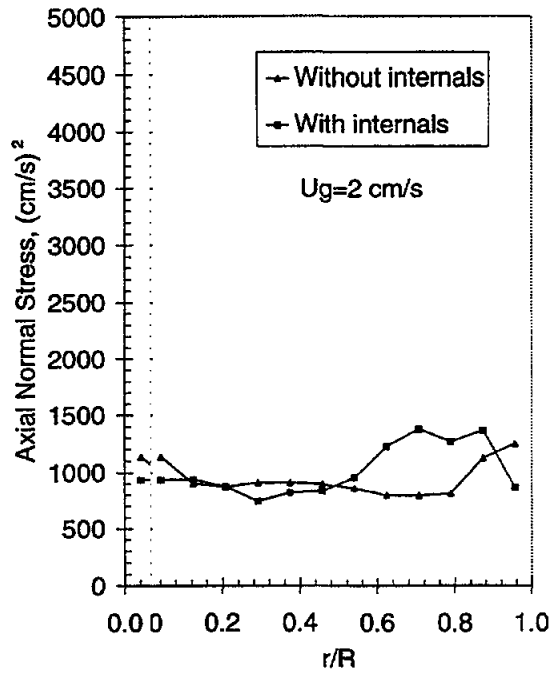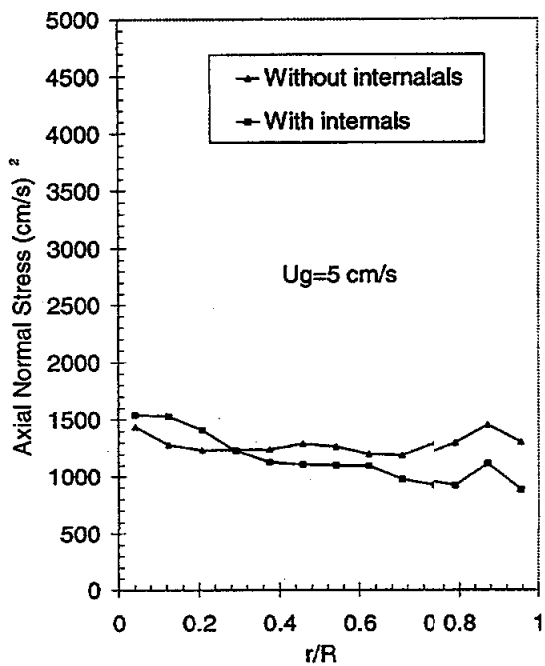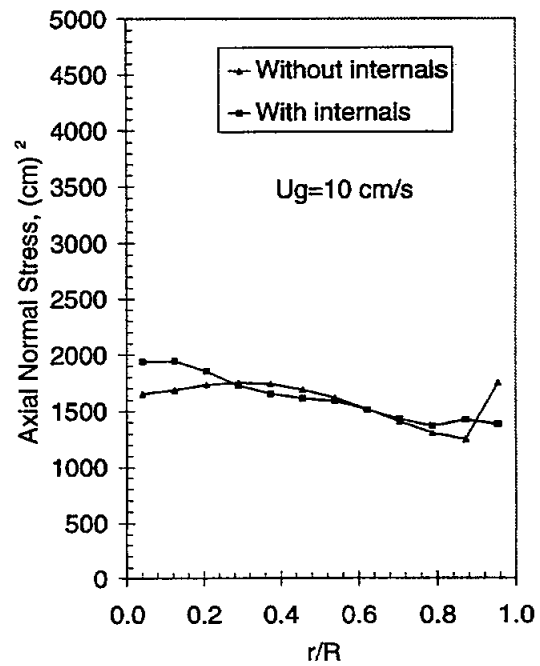
Figure 1.5 Comparison of f Axial Normal Stresses in the Columns with and without Interrrnals Using the Air-Drakeoil System
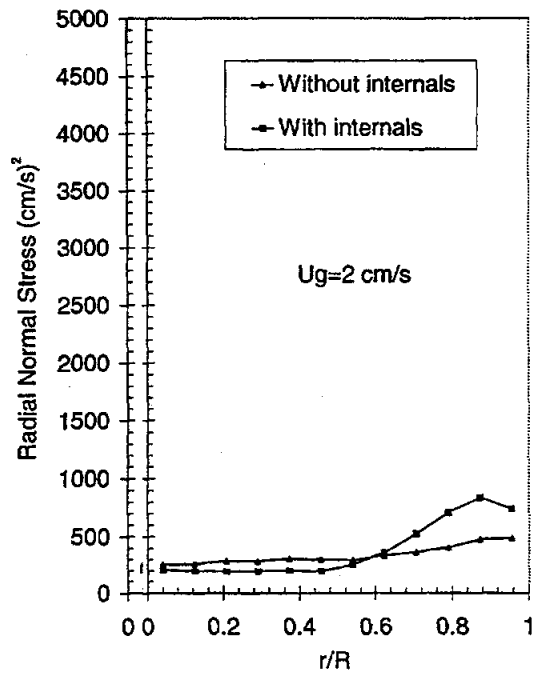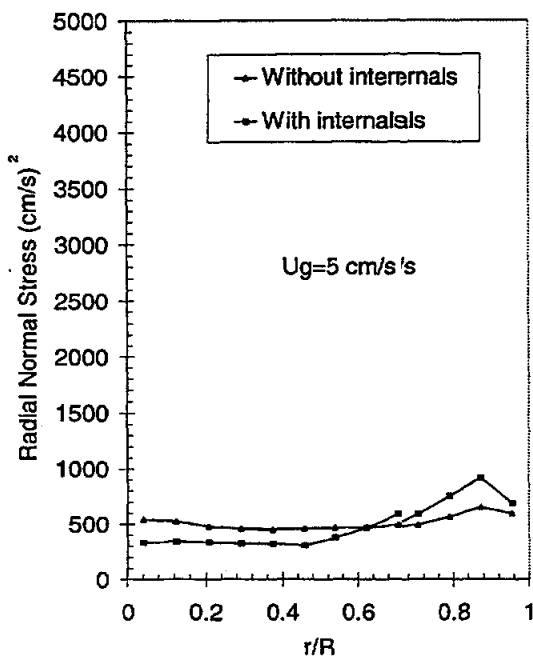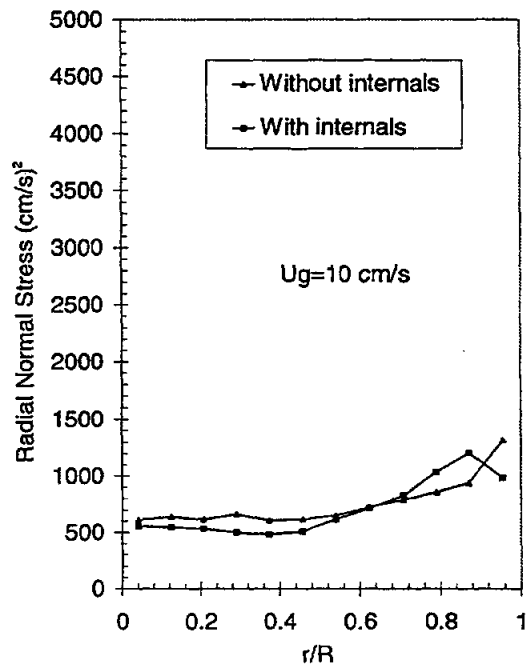
Figure 1.6 Comparison of f the Radial Normal Stresses in the Columns with and without Inteternals Using the Air-Drakeoil System

Figure 1.7 Comparison of thhe Shear Stresses in the Column with and without Internals l Using the Air-Drakeoil System
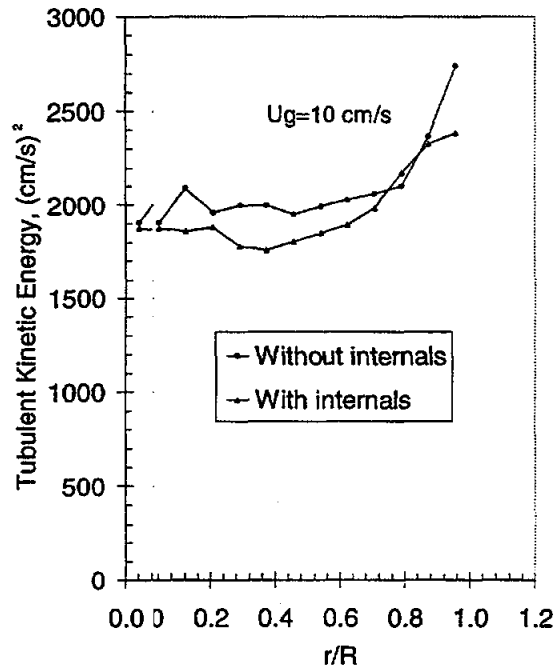
Figure 1.8 Comparison of tl the Turbulent Kinetic Energy at Gas Superficial Velocity of 10 cm/s in the Column wiwith and without Internals Using the Air-Drakeoil System

2. Establishment of the Relatitionship between the Axial Dispersion Coefficient and Parameters of the Phenomenoiological Recycle with Cross-Flow and Eddy Diffusion Model

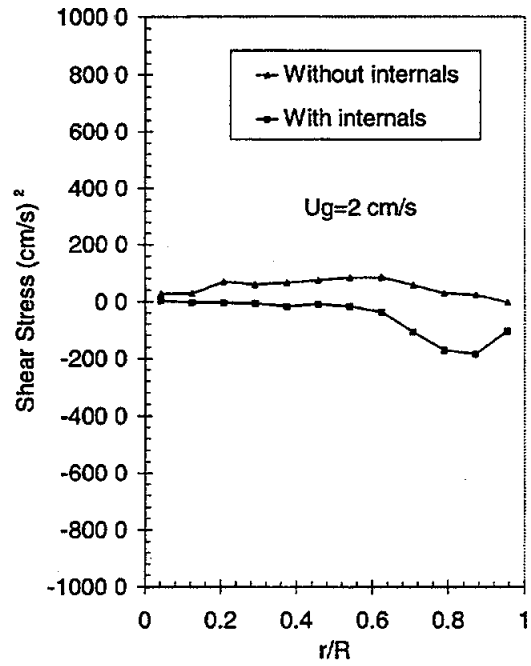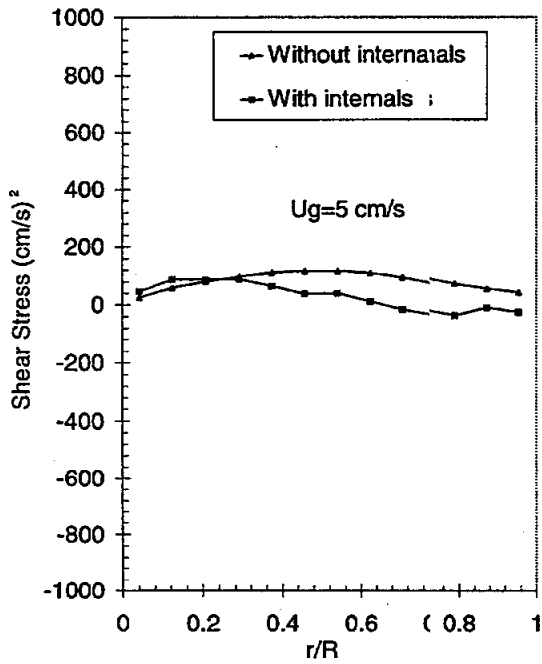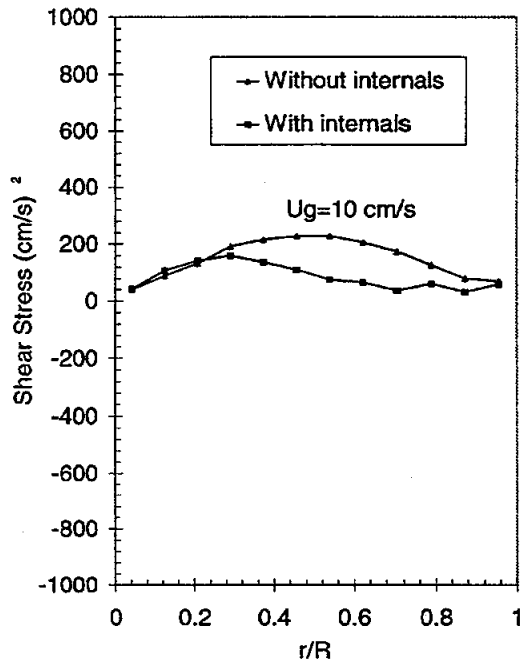A Taylor-type analysis of the twwo-dimensional convection-diffusion model for liquid mixing in a bubble column (which was deveeloped and reported in the seventh and eighth quarterly reports) was performed to establish a relalationship between the axial dispersion coefficient and the parameters of this new phenomeienologically based model. While the developed recycle with cross flow model describes the ʃ phenomena that contribute to liquid mixing in bubble columns more reasonably than the axial d dispersion model (ADM), the existence of only one parameter (the axial dispersion coefficient)t) makes the ADM still attractive to many. Therefore, we have developed a procedure to estimaiate the axial dispersion coefficient from the parameters of the phenomenologically more correcect model. For clarity, we first reintroduced the fundamental convective-diffusion model and d showed how to relate its parameters to the ADM.

2.1 Two-Dimensional Convecíction-Diffusion Model for Liquid Mixing in Bubble Columns

The fundamental two-fluid moddel mass balance equation for the local, instantaneous tracer species in phase k is as follows::

$$\frac{\partial \rho_k C_k}{\partial t} + \nabla \cdot \rho_k C_k \bar{u}_k - D_{)m} \nabla^2 C_k = 0 \tag{2.1}$$

with an interfacial jump conditionn for mass transfer across the interface:

$$\sum_{k=1}^{2} \rho_k C_k [\bar{u}_k - \bar{u}_{ki}] \cdot \bar{n}_k = 00 \tag{2.2}$$

In the above equation, the phase c density, ρ_k, for incompressible flow such as in bubble columns can be considered to be constant. t. D_m is the molecular diffusivity, which is small and will be ignored hereafter. Phasic or ensemble averaging of the above equation in an axisymmetric system, for an inert, non-volatile t tracer, yields

$$\frac{\partial}{\partial t}(\rho_k \varepsilon_k <C_k>^x) + \frac{\partial}{\partial z}\rho_k{}_k(\varepsilon_k <u_{z,k}>^x<C_k>^x + \varepsilon_k <u'_{z,k}C'_k>^x) +$$
$$\frac{1}{r}\frac{\partial}{\partial r}r\rho_k(\varepsilon_k <u_{r,k}>^x<C'_k{}_k>^x + \varepsilon_k <u'_{r,k}C'_k>^x) = <\rho_k C_k(\bar{u}_k - \bar{u}_{ki}) \cdot \nabla X_k> \tag{2.3}$$

Where $\langle\rangle^x$ represents phasic averaraging. The right-hand side of Equation 2.3 represents the term due to mass transfer across the innterface, where X_k is the phase function, defined as

$$X_k(\bar{x},t) = 1 \quad \text{if } \bar{x} \text{ is in phhase k at time t}$$
$$= 0 \quad \text{otherwise} \tag{2.4}$$

All other symbols are defined in t the nomenclature. An additional source term to represent the reaction can be added to the rightt-hand side of the equation. For the current situation, considering a non-volatile inert liiliquid tracer, the right-hand side of Equation 2.3 is set to 0. Since the model is primarily concicerned with the liquid phase, the subscript k=l, denoting the liquid phase, is dropped. In additition, all symbols denoting averaging are dropped in order to simplify notation. All variables rrepresenting the fluid dynamic parameters and the tracer concentration denote the phase-avaraged quantities.

The cross-correlation terms betwween the fluctuating velocity and tracer concentration are closed using a standard gradient diffusioion model (Hinze 1995; Tennekes and Lumley 1971; Seinfeld 1986), as

$$<u'_z C'> = -D_{zr}\frac{\partial C}{\partial r} - D_{zz}{}_z\frac{\partial C}{\partial z} \tag{2.5}$$

and

$$<u'_r C'> = -D_{rr}\frac{\partial C}{\partial r} - D_{rz}{}_z\frac{\partial C}{\partial z} \tag{2.6}$$

However, CARPT experiments slshow that the off-diagonal elements of the eddy diffusivity tensor are negligibly small. Hence,

$$D_{zr} = D_{rz} \sim 0 \tag{2.7}$$

29

Therefore

$$<u_z'C'> = -D_{zz}\frac{\partial C}{\partial z} \tag{2.8}$$

$$<u_r'C'> = -D_{rr}\frac{\partial C}{\partial r} \tag{2.9}$$

In the above equations, D_{zz} andd D_{rr} are the CARPT-measured axial and radial turbulent eddy diffusivity, respectively. Thererefore, if one ignores the inter-phase exchange terms, the final form of the model equation for flow v and mixing in the liquid phase is

$$\frac{\partial(\varepsilon C)}{\partial t} + \frac{\partial}{\partial z}(\varepsilon u_z C) + \frac{1}{r}\frac{\partial}{\partial r}(r\varepsilon u_r C) = \frac{1}{r}\frac{\partial}{\partial r}(r\varepsilon D_{rr}\frac{\partial C}{\partial r}) + \frac{\partial}{\partial z}(\varepsilon D_{zz}\frac{\partial C}{\partial z}) \tag{2.10}$$

Standard boundary conditions c can now be used with zero flux at the wall and at the centerline of the column. For the case with a continuous flow of liquid through the column, a zero gradient is assumed at the outlet, with injeiection of tracer at the inlet. Equation 2.10 represents the averaged balance equation for the non-vcvolatile liquid species, and is a transient, two-dimensional convection-diffusion equation. i. The phase (or time) averaging that has been performed to arrive at this equation refers to any tirime interval, which may be small or large.

Multiphase flows in bubble colblumns are highly transient in nature. Hence, the length of the time interval considered in the averaraging will affect the type of results obtained. Short-time averages involve averaging that is perfoorrmed over a small time interval, large enough to smooth the variations across the interface, i, but small enough to capture some of the transient structures in the flow. These transient structurees will vary in nature with the time interval of averaging. On the other hand, long-time averaginng results in a statistically stationary flow field, which is steady in time, in terms of all the fluid dylynamic variables.

Two factors are of concern herere in determining the type of averaging for the above model equation. First, since the flow γ phenomena in bubble columns is highly turbulent and random in nature, a quantitative comparisison of the fluid dynamic parameters, between model predictions and experimental measurementnts, can be made only with respect to the statistical properties of the flow field. This immediately iiimplies that time or ensemble averaging is required. Second, since the current model is consideredd in a two-dimensional axisymmetric domain, the type of boundary conditions used (zero gradient t at the centerline) will not permit the computation of physically realistic results describing the t transient structures. A true transient behavior can only be represented in a fully three-dinrmensional flow model, which can capture the inherent vortical and spiraling motion of the flow inn bubble columns.

For these reasons, we propose e considering long-time averaging for the above model equation. The various averaged quantitieies in the above equation will hence refer to long-time averaged quantities and corresponding clclosure models (Equations 2.8 and 2.9). CARPT data for the long-

time-averaged liquid velocities, u u_r and u_z, and turbulent diffusivities, D_{rr} and D_{zz}, along with CT data for the time-averaged liquid d holdup profile, can then be used as appropriate input parameters to the model.

2.2 Relationship between Axial l Dispersion Coefficient and Parameters in the Phenomenological Recycle witlth Cross Flow and Eddy Diffusion Model

A Taylor-type analysis of the funindamental, two-dimensional, axisymmetric convection-diffusion equation for liquid mixing in bubibble columns was performed to arrive at an expression for the effective axial dispersion coefficicient in terms of the two dominant factors contributing to liquid backmixing, i.e., convective recirircirculation and turbulent eddy diffusion (axial and radial). This allowed us to quantify the contritibutions of these mechanisms to overall liquid mixing in the bubble column. This analysis is s restricted to systems with low superficial liquid velocities, wherein the cross-sectional averarage liquid velocity relative to local liquid velocities is negligible. The treatment is based on a steaddy backmixing experiment in which gas and liquid are introduced at their respective flow rates co-ccurrently from the bottom of the column, and a continuous stream of liquid tracer is introduiced uniformly at the top of the column, as illustrated in Figure 2.1. For this analysis, the liquid l flow rate through the column can be as low as possible, just sufficient to ensure an outflow of)f liquid that can carry the tracer. Due to liquid backmixing, a steady axial liquid tracer concentutration profile is established in the column. This can be represented by the steady-state apapproximation of the transient, two-dimensional convection diffusion equation written as

$$\frac{1}{r}\frac{\partial}{\partial r}\varepsilon(r)D_{rr}(r)r\frac{\partial C}{\partial r} = \varepsilon(r \cdot r)u_z(r)\frac{\partial C}{\partial z} - \varepsilon(r)D_{zz}(r)\frac{\partial^2 C}{\partial z^2} \tag{2.11}$$

The above equation was written f for the well-developed region of the flow in bubble columns, where the time-averaged axial liqiquid velocity is a function of radius only, and radial velocities are zero. End effects were ignorered. This is applicable to bubble columns operating at large length-to-diameter ratios (≥ 6). BBased on the gathered experimental evidence, it was also assumed that the turbulent eddy d diffusivities in the fully developed region were a function of radial position only.
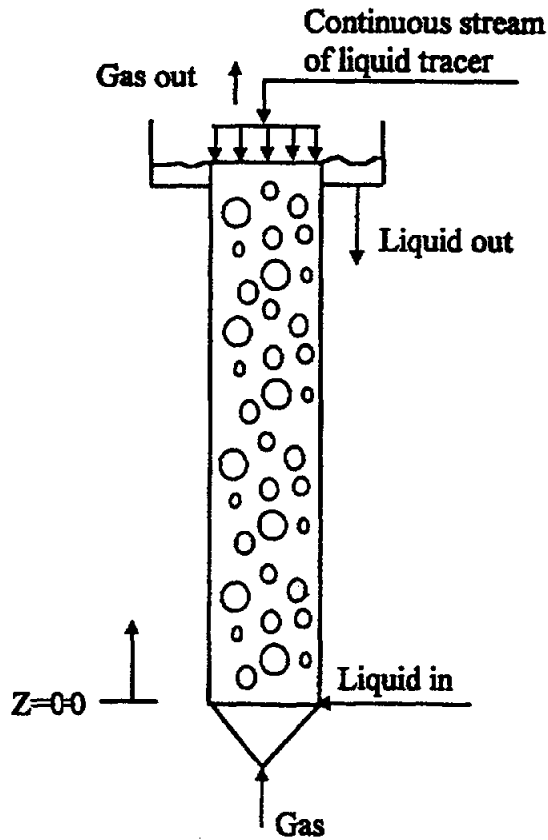
31

Figure 2.1. Steady Backmixing Liquid Tracer Experiment

The liquid tracer concerentration C(r,z) is now decomposed into two parts as

$$C(r,z) \equiv \overline{C}(z) + C C'(r) \qquad (2.12)$$

where $\overline{C}$ is a function of axial position only and $C'(r)$ is dependent on radial position only. $\overline{C}$ is the cross-sectional average liquuid concentration and, hence, is independent of radial position, r. C' represents the concentrationnn variations around the cross-sectional mean, with a cross-sectional average of zero. Simulation reessults of the steady-state, two-dimensional model, shown in Figure 2.2, indicate that C' is only a minild function of z, which is negligible when compared to $\overline{C}$. Hence, Equation 2.12 is a goodd approximation of the actual liquid tracer concentration throughout the column. Equatition 2.11 can now be rewritten as

$$\frac{1}{r}\frac{\partial}{\partial r}\varepsilon(r)D_{rr}(r)r\frac{\partial C'(r)}{\partial r} = \varepsilon(r)u_z(r(r)\frac{\partial \overline{C}(z)}{\partial z} - \varepsilon(r)D_{zz}(r)\frac{\partial^2 \overline{C}(z)}{\partial z^2} \qquad (2.13)$$

Experimental evidence from the literature (Ohki and Inoue, 1970; Myers, 1986) and simulation results (Figure 2.2) indicate an exxponential dependence of the cross-sectional mean concentration $\overline{C}$ on axial position z, as shown b by Equation (2.14):

$$\overline{C}(z) = C_0 \exp(k_z z) \tag{2.14}$$

where k_z is a constant. Therefore

$$\frac{\partial^2 \overline{C}}{\partial z^2} = k_z \frac{\partial \overline{C}}{\partial z} \tag{2.15}$$

By substituting the above result irinto Equation (2.13), we get

$$\frac{1}{r}\frac{\partial}{\partial r}\varepsilon(r)\, D_\pi(r) r \frac{\partial C'(r)}{\partial r} = \frac{\partial \partial \overline{C}(z)}{\partial z}[\varepsilon(r)u_z(r) - \varepsilon(r)D_{zz}(r)k_z] \tag{2.16}$$

With a Taylor-type analysis (afterr double integration over r) having a symmetry condition at the center and zero flux at the wall, ththe following equations are obtained:

$$C'(r) = \frac{d\overline{C}(z)}{dz} I2(r) \tag{2.17}$$

where

$$I2(r) = \int_0^r \frac{I(r')}{r'\varepsilon(r')D_\pi(r')}dr'r' \tag{2.18}$$
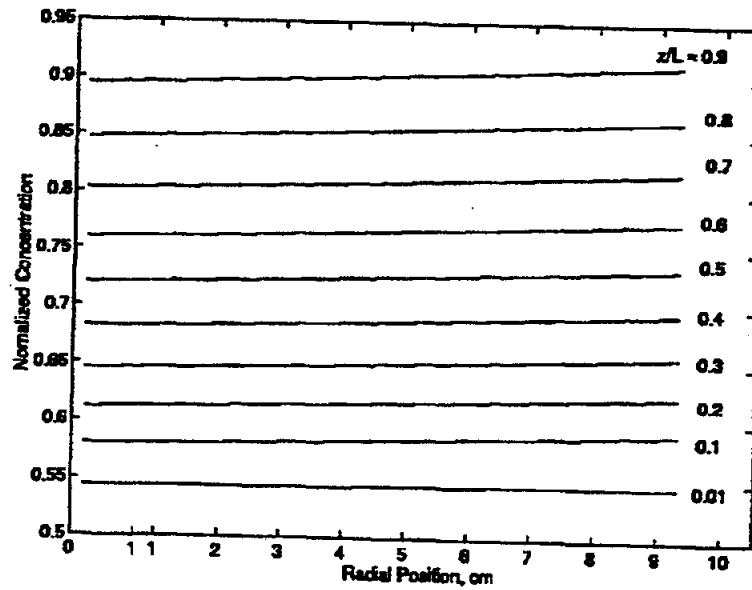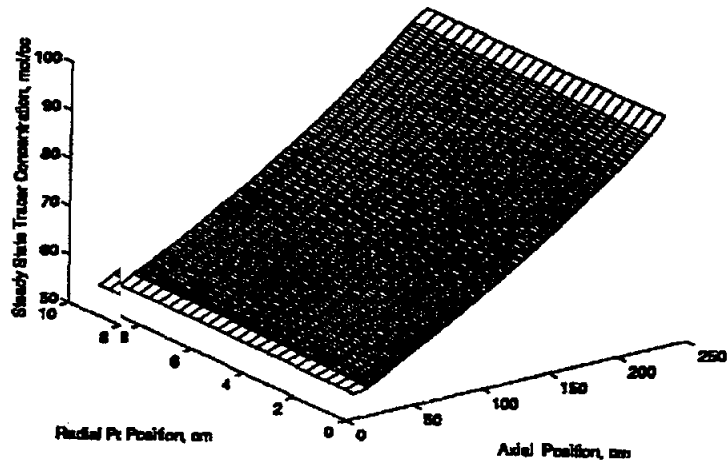
and

Figure 2.2.   Simulation n Results for the Steady State Two Dimensional Convection Diffusion Moodel

$$\int_0^r r\varepsilon(r')[u_z(r') - D_{zz}(r')k_z k_z]dr' \qquad (2.19)$$

An average flux for a cross-section of the column can now be defined as

$$J = \frac{\int_0^R r\varepsilon(r)u_z(r)C(r,z)dr}{\int_0^R r\varepsilon(r)dr} - \frac{\int_0^R \int_0^R \varepsilon(r)rD_{zz}(r)dr}{\int_0^R r\varepsilon(r)dr}\frac{\partial\overline{C}}{\partial z} = T_1 - T_2 \qquad (2.20)$$

Substituting Equation (2.12) for $C(r,z)$ in the first term of Equation (2.20), the integral involved can be dropped, giving the followwing expression for T1:

$$T1 = \frac{\partial\overline{C}(z)}{\partial z}\frac{\int_0^R r\varepsilon(r)u_z(r)I2(r)r dr}{\int_0^R r\varepsilon(r)dr} = -D_{Taylor}\frac{d\overline{C}_z}{dz} \qquad (2.21)$$

The second term in Equation 2.200 can be written as

$$T2 = \overline{D}_{zz}\frac{d\overline{C}_z}{dz} \qquad (2.22)$$

Therefore,

$$J = -\frac{\partial\overline{C}(z)}{\partial z}[D_{Taylor} + \overline{D}_{zz}] \qquad (2.23)$$

$$D_{eff} = D_{Taylor} + \overline{D}_{zz} \qquad (2.24)$$

From the above analysis it is possssible to estimate the contributions of convection (Taylor dispersion) and turbulence to the e one-dimensional axial dispersion coefficient. The Taylor dispersion coefficient, D_{taylor}, and d the averaged axial eddy diffusivity, $\overline{D}_{zz}$, can be directly evaluated from turbulent diffusiviivities and liquid velocities obtained by CARPT experiments, and from the gas holdup profiles obtaiained by CT. This will be discussed in a subsequent quarterly.

2.3 Nomenclature

C	liquid tracer concentration, mol/cm^3
$\overline{C}$	cross-sectional averaged concentration, mol/cm^3
C'	concentration variation around the mean, mol/cm^3
C_0	constant in Equation (2.14)
$\mathbf{D}$	turbulent eddy diffusivity tensor
D_{eff}	effective axial dispersion coefficient defined by Equation (2.24)
D_{ax}	axial dispersion coefficient, cm^2/s
$D_{rr}, D_{zz}, D_{\theta\theta}$	diagonal elements of eddy diffusivity tensor, cm^2/s
$D_{rz}, D_{r\theta}, D_{z\theta}$	off-diagonal elements of eddy diffusivity, cm^2/s
D_{Taylor}	Taylor dispersion coefficient, cm^2/s
$\overline{D}_{rr}, \overline{D}_{zz}$	averaged radial and axial eddy diffusivities, cm^2/s
$I2(r), I(r)$	functions defined by Equation (2.18) and (2.19)
J	average flux across the cross section of the column, $\text{mol/cm}^2/\text{s}$
k_z	constant in equation (2.14)
$\vec{n}_k$	unit normal vector in phase k
R	coordinate in r direction, cm
T	time, s
T_1, T_2	functions defined by Equations (2.21) and (2.22)
u_r, u_z	velocity in r and z direction, cm/s
$\vec{u}$	Eulerian velocity, cm/s
$\vec{u}_k$	velocity vector in phase k, cm/s
$\vec{u}_{ki}$	interfacial velocity vector, cm/s
u'_r, u'_z	fluctuation velocity in r and z directions, cm/s
$\vec{x}$	position vector
X_k	phase (k) function
Z	coordinate in z direction, cm/s

Greek symbols

ε	phase holdup
ε_k	holdup of phase k
ρ_k	density of phase k

2.4 References

1. Myers, K. J., "Liquid Phase MMixing in Churn Turbulent Bubble Columns," D. Sc. Thesis, Washington University, St. LLouis, MO, 1986.
2. Ohki, Y. and H. Inoue, "Longgitudinal Mixing of the Liquid Phase in Bubble Columns," Chem. Eng. Sci., Vol. 25, 1-116 (1970).
3. Hinze, J. O., "Turbulence," MMcGraw-Hill, New York (1975).
4. Seinfeld, J. H., "Atmospheric c Chemistry and Physics of Air Pollution," Wiley Publications, New York (1986).
5. Tennekes, H. and J. L. Lumleyey, "A First Course on Turbulence," The MIT Press, Cambridge (1972).

3. Progress in Evaluation of thae Momentum Balance Equation for Bubble Columns Using CARPT and CT Measurementsts

3.1. Introduction

Experimentally determined gas hooldup and Reynolds stresses in a 14-cm-diameter bubble column were used to evaluate the e dominant terms in the radial momentum balance equation using a two-fluid model approachh. (The detailed analysis was reported in the 10th quarterly report). The following assumptio:ons were made in the formulation of the problem:
1. Viscous effects are negligible e for both phases.
2. Gas inertial effects are negligizible.
3. Mean radial drag force is neglzligible.
4. Wall effects are not included. l.
5. Radial components of the virtrtual mass and lift forces are negligible.
6. Gas-liquid velocity correlationns are small.

These assumptions resulted in theie following simplified radial momentum balance equation:

$$\frac{d}{dr}\left(r\alpha^l \overline{u_r'^l u_r'^l}\right)^{\overline{l}} = \alpha^l \overline{u_\theta'^l u_\theta'^l} + \frac{r\overline{F_r^T}}{\rho^l(\alpha^l - 1)} \tag{3.1}$$

where $\overline{F_r^T}$ is the fluctuating compponent of the drag force in the radial direction. Two models were used to evaluate the momenntum budget in the bubble column. First, the fluctuating component of the radial drag forcice was ignored. This yielded the following equation:

$$\frac{d}{dr}\left(r\alpha^l \overline{u_r'^l u_r'^l}\right) = \alpha^l \overline{u_\theta'^l u_\theta'^l} \tag{3.2}$$

In the second model, an approachh for modeling the turbulent drag force, as proposed by Jakobsen (1993) and Sannaes (1997), was uused. The resulting expression for the turbulent drag force was inserted in eq. (3.1), and the folloowing equation was obtained:

$$\frac{d}{dr}\left(r\alpha^l \overline{u_r'^l u_r'^l}\right) = \alpha^l \overline{u_\theta'^l u_\theta'^l} - \frac{3}{4}\frac{r}{\rho^l}\alpha^l \frac{\mu_l}{d_s^2} C_D \left(\frac{d_p}{v_l}\right)^2 \frac{\overline{w_z}}{\text{Re}_p} \overline{w_z' w_r'} \tag{3.3}$$

By plotting the left-hand side (L.I.H.S.) of eq. (3.2) and eq. (3.3) versus the right-hand side (R.H.S.), the accuracy of the assuuumptions made in deriving the above equations was evaluated

for both models. The analysis s showed a discrepancy near the wall between the two sides for both equation (3.2) and equation (3.3.3). The results of this analysis for a 14-cm-diameter bubble column at gas superficial velocicities of U_g = 4.8 and 12 cm/s, and a 19-cm-diameter column at U_g = 4.8 cm/s have been reported il in the previous quarterly report no. 10.

This analysis was repeated for ɛ a new set of experimental data obtained in a 10-cm-diameter bubble column at U_g = 2 and 8 8 cm/s. In these experiments, both holdup and velocity field were measured in the same system (s(same water, same impurities, etc.), unlike the previously treated data for which holdup and veloʋocity measurements had been performed during different measurement campaigns.

Figure 3.1 shows the results obibtained from equation (3.2) for the 10-cm-diameter column. In this figure, the L.H.S. of equation (:(3.2) is plotted versus the R.H.S. It can be seen that there is a significant mismatch between tl the two sides of eq. (3.2) for U_g = 8 cm/s, while a reasonable agreement is obtained for U_g = = 2 cm/s. These results confirm the previously reported observations.

In this report, the possible sourʋrces of the observed discrepancies are discussed.

3.2 Discussion

The first step in searching for tlthe cause of the above-mentioned discrepancies was to determine the validity of the initial assumpnptions 1 to 5. These were checked and confirmed by the following arguments:
1. Turbulent viscosities are ororders of magnitude higher than molecular viscosities. The typical values of the terms correspoonding to viscous stresses in the radial direction are on the order of 0.0001 to 0.01 cm^2/s^2 coompared to the typical values of the Reynolds stress terms, which range from 25 to 400 $cm^2/s's^2$.
2. Gas density is three orders ɕ of magnitude (1/1000) smaller than liquid density in an air-water system at ambient pressure ɛ and temperature. Hence, gas inertial effects are negligible.
3. Mean radial slip velocity is s negligible, and the momentum exchange coefficient is small, which makes the mean dragɑg force term negligible compared to the Reynolds stress terms. The typical values of the raɑadial drag force term are about 1 cm^2/s^2, while the typical values of the Reynolds stress terms rɑrange from 25 to 400 cm^2/s^2 for different cases. Thus, the mean radial drag is negligible.
4. The analysis is performed bby using velocity and holdup data only in the region from 0 to 0.85 dimensionless radius; hencɛce, wall effects are not captured and thus should not influence our analysis.
5. Radial components of addeɕed mass and lift forces are also negligible for the same reasons as in the case of the mean radiɟlial drag force, discussed in (3) above.

The following additional investstigations were also conducted to detect the possible sources of error related to the assumption ɑ of fully developed flow and variability in determination of the Reynolds stress and gas hold-uʃup profiles, as well as the uncertainty in estimation of the gas velocity profile.

1. The fully developed flow conndition requires that the velocity (and hence, the Reynolds stress) profiles do not vary in the axiial direction. In order to evaluate the validity of this assumption, the Reynolds stress profiles wwere examined at different heights in the middle section of the column and compared for all d cases. All the profiles showed similar increasing or decreasing trends, and discrepancies in ththeir shape and magnitude were relatively small. This fact is illustrated in Figures 3.2 and 3 3.3, where the normal Reynolds stress profiles at different heights in the middle section α of the column are compared in a column with $D_c = 14$ cm and at $U_g = 12$ cm/s. Hence, variatidions in Reynolds stress profiles cannot explain the observed discrepancies.

2. The uncertainty in measured F Reynolds stresses was examined next. The error bars for all of the radial profile data points a are comparable (Degaleesan, 1997), and this is not the source of the observed differences. Figigure 3.4 shows an example of the uncertainty in determination of the Reynolds stresses for the c case of $D_c = 14$ cm.

3. The radial gas holdup profile ♭ was examined next. The following equation was used for smoothing the measured gas h holdup profiles:

$$\alpha_g(\xi) = \tilde{\alpha}\left(\frac{mm+2}{m}\right)(1 - c\xi^m) \qquad (3.4)$$

A careful analysis of the gas h holdup profiles for different axial positions in the so-called fully developed section of flow yielelded the values of m and c, which vary significantly with height. Different holdup profiles werere tested, and it was found that the match between the two sides of eq. (3.1) is very sensitive tdo the holdup gradient, especially at high superficial gas velocity. For all three cases, the deviatition between the R.H.S. and the L.H.S. of eq. (3.1) starts at about 0.6 to 0.7 in dimensionless raadius, which matches the break point of the holdup profiles (typical values of m range froom 2.5 to 4 in the case of 12 cm/s superficial gas velocity in the 14-cm column). By increasinpng the coefficient m from 3.5 (the average value) to 4.5, a good agreement could be found for r the case of high gas superficial velocity. The effect of m on equation (3.2) for $D_c = 14$ cm n and $U_g = 12$ cm/s is shown in Figure 5. The value of c does not play a significant role in the cicalculations, since we have excluded the wall from our analysis. The change in the holdup pararameters had a much smaller effect in the cases with lower superficial gas velocities. Thihis fact is illustrated in Figure 6 for $D_c = 14$ cm and $U_g = 4.8$ cm/s by examining the resultsis for $m = 3$ and $m = 4.5$. Hence, the radial gas holdup profile variations with axial position n may account for some of the observed mismatch in the radial momentum balance.

4. The sensitivity of the results tcto the assumed gas velocity profiles was examined, and was found to be only a small sourarce of error, as illustrated in Figure 3.7, where the results have been plotted for two different ,t gas velocity profiles.

5. Finally we examined our assuuumption 6 of negligible gas-liquid correlation. Ignoring the correlations between gas and l liquid velocities that arise in the formulation of the turbulent drag force by this method seeiems to be unjustified. The addition of these terms can change the sign of the turbulent drag forcice. Unfortunately, experimental methods do not exist at present for the measurement of these c correlations. Therefore, the development of a closure model for these correlations is an importrtant but difficult task that should be considered in the future work on CFD simulations usiiing the two-fluid model approach. A theoretical approach proposed by Simonin (1996) c can be used for determination of the gas-liquid velocity

correlations. In the simpleiest form of this approach, it can be assumed that the particles (bubbles) are only locally e entrained by the fluid, hence, this method is called the "local entrainment approach." Inn this approach, the standard fluid Lagrangian time-scale, the fluid Lagrangian time-scale meaasured along the particles path (i.e., the Lagrangian time scale "seen" by the particles) anad the particle relaxation time should be known. The gas-liquid velocity covariance can be e calculated from this information and the individual phase velocity fields. The gas-liquid veloocity correlations are expressed in terms of this covariance, and the gas and liquid phase velocixity gradients, by using a Boussinesq type closure model. Our preliminary analysis using g this model has shown that the change in the turbulent drag force due to consideration of the e gas-liquid velocity correlations is small. However, the uncertainty in determination of differeient time scales, and the difficulty in checking the validity of the model assumptions, makes;s the final judgment difficult. The description of the method for determination of gas-liquidd velocity covariance using the experimental data will be the subject of the future reporirt, where this matter will be discussed in more detail.

3.3 Conclusion

In conclusion, it seemsns that the error in estimation of hold-up profiles has considerable effect on the match between i the two sides of the momentum balance in the radial direction, especially at higher superficiallal gas velocity.

The lack of ability to o measure gas-liquid velocity correlations make the evaluation of their relative importance in dettermination of the turbulent drag force a difficult task.

The numerical error in n determination of the derivative term on the L.H.S. of eq. (3.1) can be another important source (of error. More experimental points are needed close to the wall, where the gradients are steepeuer. A careful analysis should also be made of the effect of filtering on determination of Reynolds s stresses by the CARPT technique.

3.4 Nomenclature

C_D	Drag force ccoefficient
D_p	Bubble diammeter
D_s	Sauter meann diameter
F	Drag Force :
R	Radial coordrdinate
Re	Reynolds nuumber
U	Velocity
W	Slip velocityty

Greek letters
α	Hold-up
μ	Viscosity
ρ	Density
θ	Azimuthal c·coordinate

Subscripts
R	Radial coordrdinate

Z	Axial coordinate
I	General space e coordinate
θ	Azimuthal cooordinate

Superscripts

$^{-}$	Mean
$'$	Fluctuation ab.bout mean
L	Liquid
G	Gas
T	Turbulent
D	Drag

3.5 References

1. Degaleesan S., "Fluid Dynnamic Measurements and Modeling of Liquid Backmixing in Bubble columns", D.Sc. Theιesis, Washington University, St. Louis (1997).
2. Jakobsen S.A., "On the Moodelling and Simulation of Bubble Column Reactors Using Two-Fluid Model", Dr. Ing. Thesisis, Norwegian University of Science and Technology, Trondheim (1993).
3. Kumar S. B., "Computed To'omographic Measurements of Void Fraction and Modeling of the Flow in Bubble Columns", ΓD.Sc. Thesis, Washington University, St. Louis (1994).
4. Sannaes B.H., "Solid Movemment and Concentration Profiles in Column Slurry Reactors", Dr. Ing. Thesis, Norwegian Univiversity of Science and Technology, Trondheim (1997).
5. Simonin O., "Combustion aιand Turbulence in Two-Phase Flows - Continuum Modelling of Dispersed Two-Phase Flows's", von Karman Institute for Fluid Dynamics, Lecture series 1996-02, 1996.
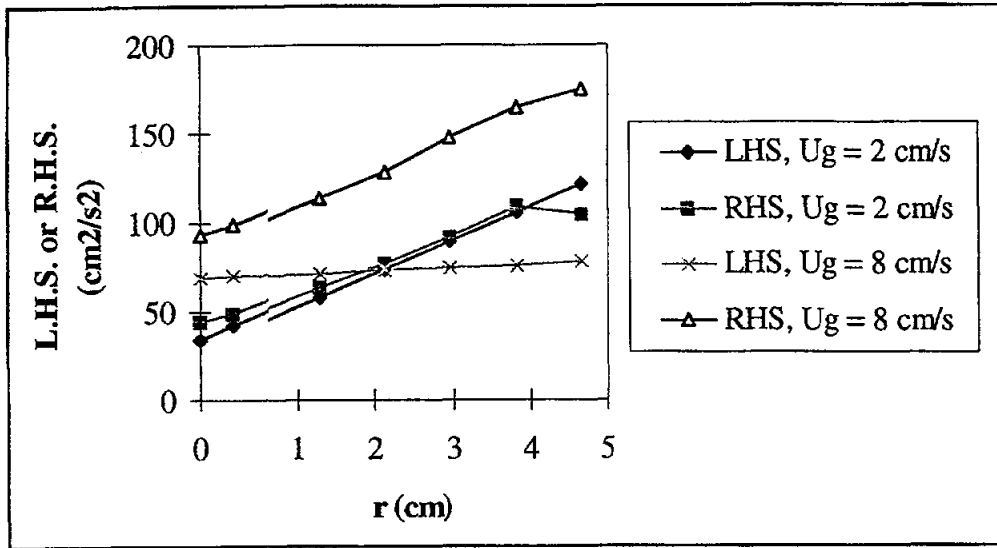
Figure 3.1. The analysis of rradial momentum balance for a 10 cm diameter bubble column using equation (3.2).
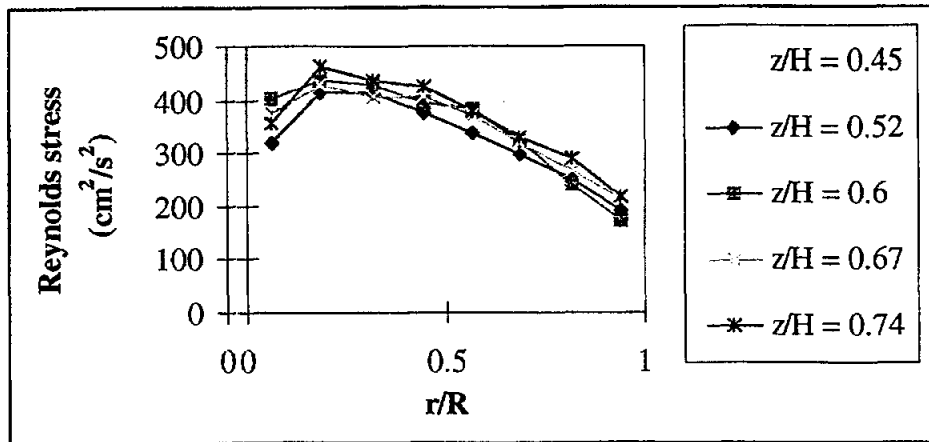

Figure 3.2. Radial profiles obf the normal Reynolds stresses in the radial direction, $\overline{u_r'^l u_r'^l}$, at different axial positions ($D_c = 14$ cm and $U_g = 12$ cm/s).
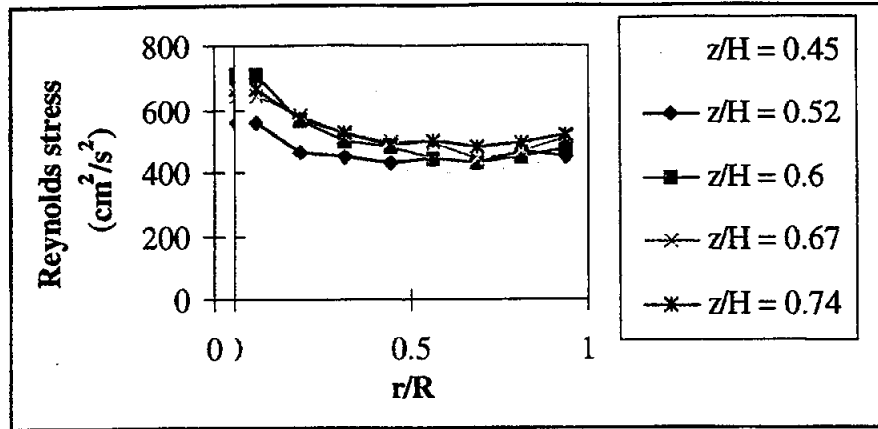
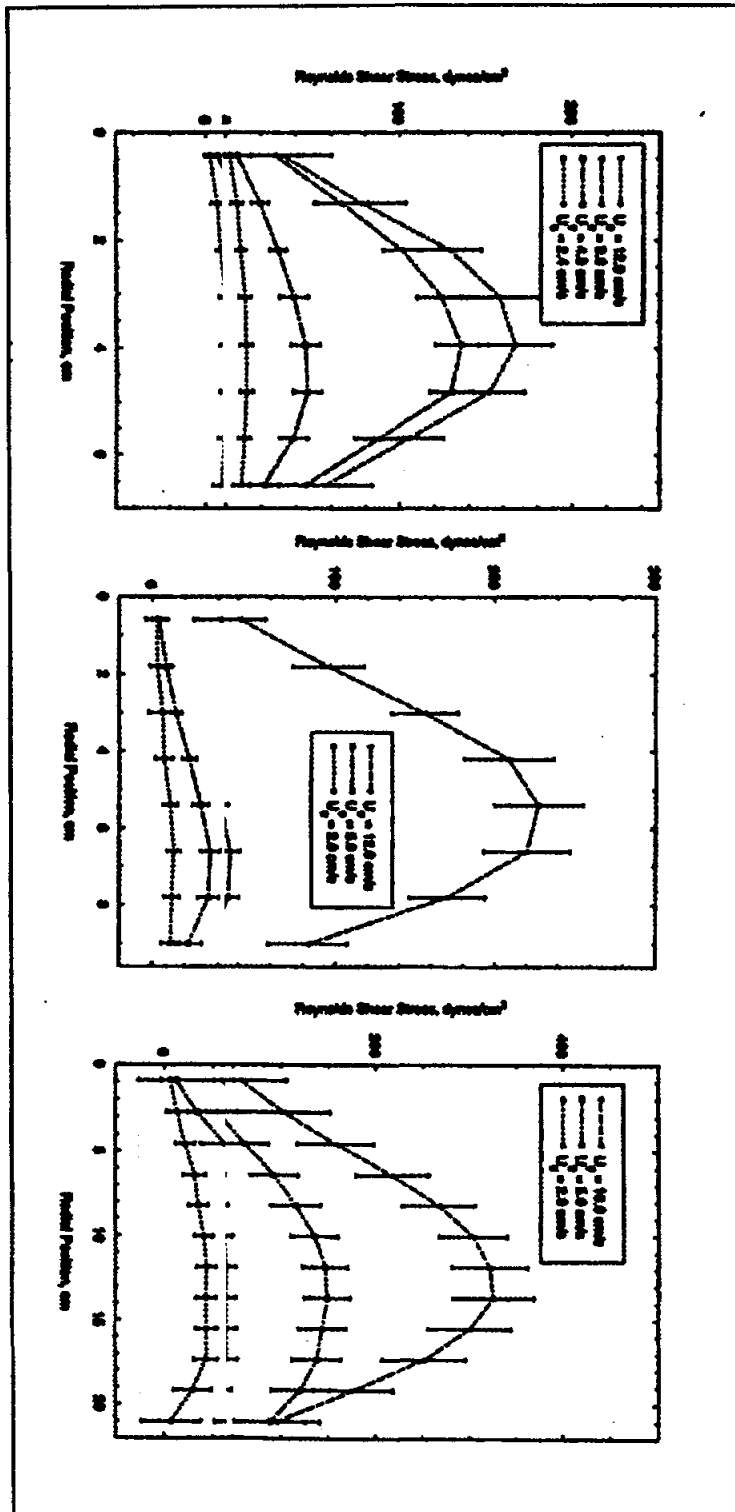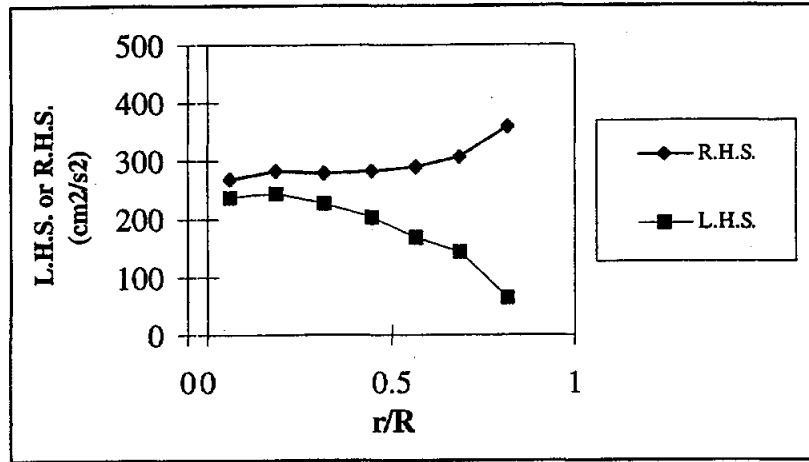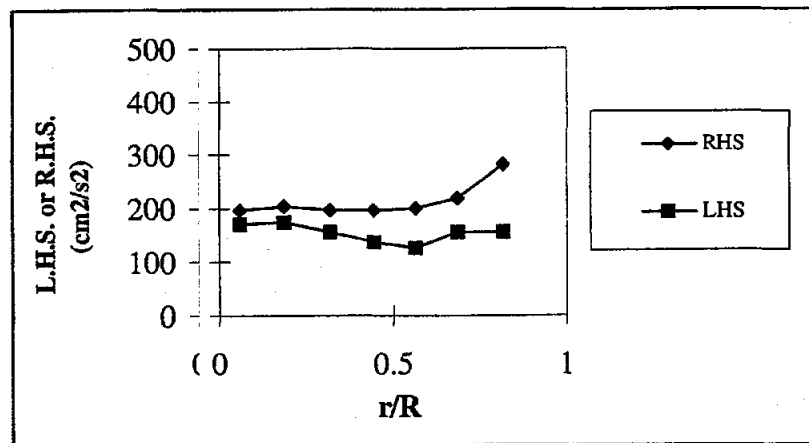**Figure 3.3.** Radial profiles o of the normal Reynolds stresses in the azimuthal direction, $\overline{u_\theta'^l u_\theta'^l}$, at different axial positions ($D_c = 14$ cm and $U_g = 12$ cm/s).

Figure 3.4. Spread of Ґ Reynolds stress data about the average profile for CARPT measurements in (a) $D_c = 114$ (a) $D_c = 19$ (b) and $D_c = 44$ (c) cm bubble columns at $U_g = 2$ to 12 cm/s
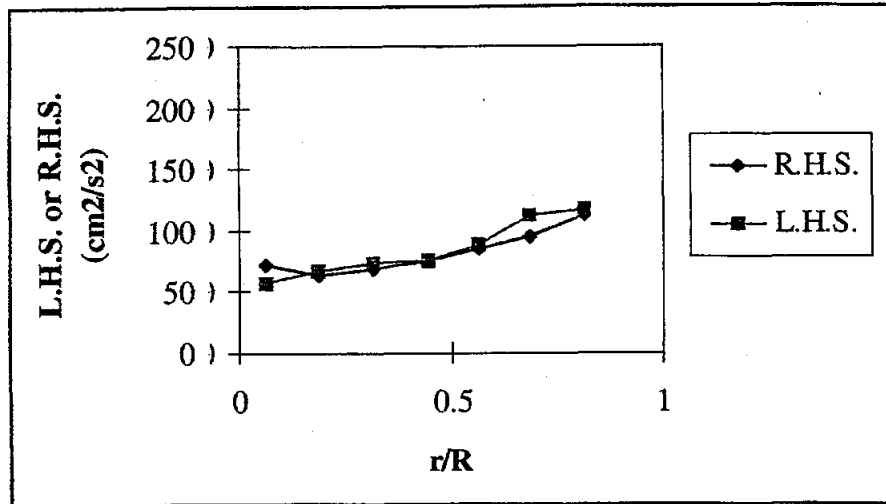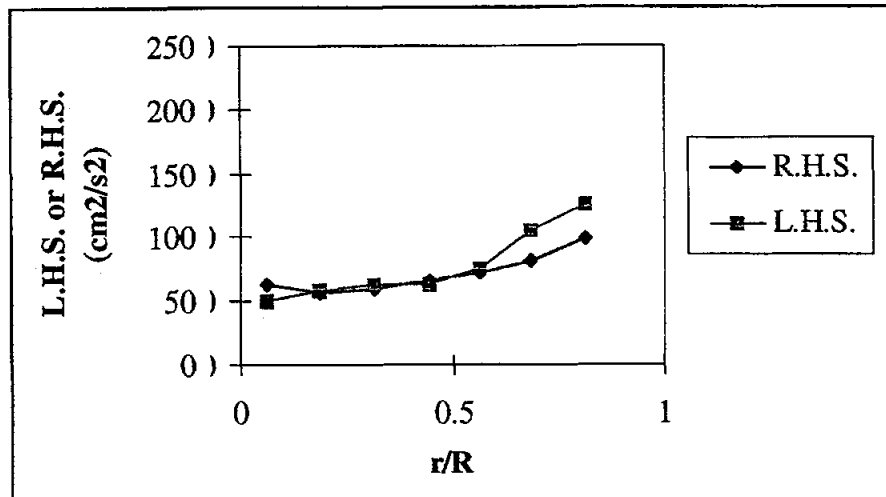
(a)

(b)

Figure 3.5. RHS and LHSS of equation (3.2) plotted for $D_c = 14$ cm and $U_g = 12$ cm/s using holdup profildes with different values of m (a) $m = 3.5$ (b) $m = 4.5$

(a)

(b)

Figure 3.6. RHS and LHHS of equation (3.2) plotted for $D_c = 14$ cm and $U_g = 4.8$ cm/s using hold-up prcofiles with different values of m (a) $m = 3$ (b) $m = 4.5$
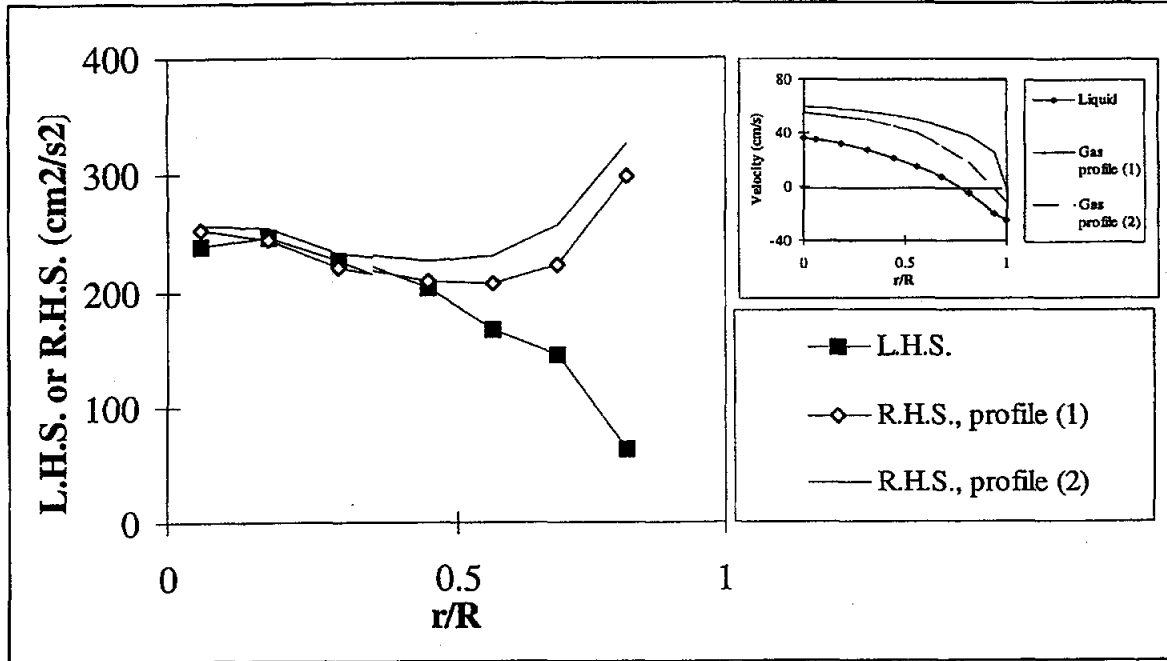
Figure 3.7. Effect oof gas velocity profile on the RHS of equation (3.1)
f for $D_c = 14$ cm and $U_g = 12$ cm/s